

Microscopic theory of vibronic dynamics in linear polyenes

L. Arrachea¹, A. A. Alliga², and G. E. Santoro¹¹: Scuola Internazionale Superiore di Studi Avanzati (SISSA) and Istituto Nazionale per la Fisica della Materia (INFM)
(Unità di Ricerca Trieste-SISSA), Via Beirut 4, I-34014 Trieste, Italy² Centro Atomico Bariloche, (8400) Bariloche, Argentina.

(October 9, 2021)

We propose a novel approach to calculate dynamical processes at ultrafast time scale in molecules in which vibrational and electronic motions are strongly mixed. The relevant electronic orbitals and their interactions are described by a Hubbard model, while electron-phonon interaction terms account for the bond length dependence of the hopping and the change in ionic radii with valence charge. The latter term plays a crucial role in the non-adiabatic internal conversion process of the molecule. The time resolved photoelectron spectra are in good qualitative agreement with experiments.

PACS Numbers: 31.25.Qm, 31.50.Gh, 33.60.-q, 31.70.Hq

Photoexcitation in polyatomic molecules leads to the rapid mixing of vibrational and electronic motions, including charge redistribution and energy flow in the molecule. This non-adiabatic coupling is essential in photochemical processes [1], in photobiological processes, such as those involved in vision [2], and in molecular electronics [3].

The progress in the technology of laser pulses has triggered the development of a new generation of spectroscopies devoted to the investigation of ultrafast phenomena. Beautiful experiments have been recently reported on the study of ultrafast non-adiabatic processes in isolated molecules [4,5]. Time-resolved photoelectron spectroscopy (TRPS) has been used to follow the vibronic dynamics of all-trans 2,4,6,8 decatetraene [5]. In this molecule, the electronic ground state is the singlet S_0 ($1^1 A_g$), while the first optically allowed excited state, S_2 ($1^1 B_u$), has an energy higher than the first excited "dark" singlet S_1 ($2^1 A_g$). A laser pulse (pump) prepares the molecule in a vibrationally hot wave packet involving the state S_2 . The packet evolves and its time evolution is probed by photoexciting an electron and analyzing the ensuing spectra at subsequent times. The population of the "dark" band, associated with the S_1 electronic state increases with time, as a consequence of a non-adiabatic internal conversion between vibrational and electronic excitations. Such a process lasts a few hundred femtoseconds, and is a manifestation of the failure of the adiabatic description.

The aim of any theory in this field is to relate experimental spectroscopical data with the basic microscopic interactions of the system. This task is particularly difficult in the present case. A theory describing the experiments should start from a model which includes both electron-electron correlations as well as electron-phonon couplings, and should treat the latter beyond the adiabatic approximation. So far, to the best of our knowledge, time dependent photoemission spectra for such non-adiabatic internal conversion processes have never

been calculated on the basis of a microscopic model. Previous theoretical work on the internal conversion process is based on semiempirical models for the relevant energy surfaces, supplemented by phenomenological couplings between them [7].

The goal of this Letter is to describe the whole process behind a TRPS experiment [5] (laser pump followed by a dynamical internal conversion, probed by the ensuing time-dependent photoemission spectra), using a minimal microscopic model in which both electron-electron and electron-phonon interactions are exactly taken into account. Our results show a good qualitative agreement with the experimental findings [5], and provide a link between these and the basic underlying microscopic interactions.

The model we study is based on a formal separation of the hybridized s and p orbitals lying in the plane of the molecule (see Fig. 1(a)), and the p-orbitals perpendicular to it. The former are those with the larger contribution to the chemical bond and vibration dynamics. The latter are those involved in the low-energy excitations of interest to us, and are described by a Hubbard Hamiltonian. Its key ingredient is a strong local Coulomb interaction U . Electron-phonon coupling terms are included, as derived from an expansion of the electron-ion interaction up to first order in the ionic displacements relative to the equilibrium positions [6]. The model reads:

$$\begin{aligned}
 H = & \sum_{i=1}^X \sum_{\sigma=\uparrow,\downarrow} \epsilon_i^\sigma (f_{i\sigma}^\dagger - f_{i\sigma})^2 + \sum_{i=1}^X \sum_{\sigma=\uparrow,\downarrow} \epsilon_i^\sigma (f_{i\sigma}^\dagger - f_{i\sigma})^2 + H_{\text{ph}} \\
 & + U \sum_{i=1}^X n_{i\uparrow} n_{i\downarrow} + g^0 \sum_{i=1}^X (u_{i+1} - u_i) (q_i + q_{i+1}) \\
 & + \frac{K}{2} \sum_{i=1}^X (u_i - u_{i+1})^2 + \frac{1}{2m} \sum_{i=1}^X p_i^2; \quad (1)
 \end{aligned}$$

where $i = 1, \dots, L$ labels the orbitals of the C atom s , $f_{i\sigma}^\dagger$ creates an electron with spin σ at site i ,

$n_i = f_{i\uparrow}^\dagger f_{i\uparrow}$ is the corresponding number operator, and $q_i = 1 - n_{i\uparrow} - n_{i\downarrow}$ is the net charge at site i . u_i are the ionic displacements with respect to the equilibrium positions, and, for simplicity, the vibration dynamics has been assumed to be that of a one dimensional chain of ions (the CH units) of mass m with a nearest-neighbor harmonic constant K . Two electron-phonon interaction terms have been included in Eq. (1), with coupling constants labeled by g and g^0 . The g -term is quite standard and accounts for the fact that the magnitude of electronic nearest-neighbor hopping becomes weaker or stronger as the bond stretches or compresses, respectively. The g^0 -term, with $g^0 > 0$, accounts for the contraction (expansion) of the bond upon removal (addition) of an electron. Such a term is a consequence of the dependence upon the valence charge of the spread of the wave functions (particularly the orbitals), a spread which in turn modifies the bond lengths.

For sake of simplicity, and in order to be able to numerically solve exactly the Hamiltonian, we consider a molecule with $L = 4$ C atoms. The vibrational motion of the molecule for $g = g^0 = 0$ can be described in terms of three normal modes, e_a , e_b , and e_c , oscillating with frequencies $\omega_a = \frac{1}{2} \sqrt{(2 + \sqrt{2})K/m}$, $\omega_b = \frac{1}{2} \sqrt{(2 - \sqrt{2})K/m}$, and $\omega_c = \frac{1}{2} \sqrt{2K/m}$, as sketched in Fig. 1(b). The mode e_b will not be included, since it describes a uniform dilatation or contraction of the molecule, which should have a small coupling with the electrons in a larger molecule.

In order to show that the Hamiltonian (1) represents the minimum model containing the relevant ingredients to describe the physics of decatetraene, we begin by discussing the role played by each interaction term within the adiabatic picture.

Role of U . The role of electronic correlations in the excitation spectrum of polyenes has been already discussed [9,10]. Here if U were neglected, the optically allowed S_2 state would have a lower energy than the dark S_1 state, while $(U=t_0)^{1/2}$ leads to the observed ordering of both singlet excitations. Given the reasonable estimate of $t_0 = 2$ eV for the electronic hopping [8], we find that the value of U that best fits the data on decatetraene is $U = 4.2$ eV.

Role of g . The electron-phonon interaction g is a standard ingredient of the Pariser-Parr-Pople-Pierls (PPPP) model [9,10], crucial in explaining dimerization effects. The coupling between the electrons and the e_a mode (the dimerization mode) leads to different equilibrium lengths for C-C and C=C bonds, alternating short and long bonds. From experimental data [11] we took $\omega_a = 0.2$ eV (which implies $K = 36$ eV/Å² and $\omega_c = 0.15$ eV). A value for $g = 3$ eV/Å is then calculated by fitting the experimentally observed difference in bond-lengths [11]. Setting for the time being $g^0 = 0$, one can study the Born-Oppenheimer (BO) surfaces corresponding to the three lowest energy singlets S_0 , S_1 , S_2 , as functions of

the normal mode coordinates e_a and e_c (see Fig. 1(c)). The position of the minimum of the ground state BO surface, occurring at a finite $e_a > 0$, reflects the dimerization. It is also evident from Fig. 1(c) that the electron-phonon coupling introduces anharmonicity in the BO energy surfaces leading to the occurrence of level crossings in the excited states, known as conical intersections [6]. The S_2 singlet is odd under space inversion while the S_1 is even. The conical intersection between both states is a central feature of the physics we want to describe. Note that the e_a mode is even under inversion, while e_c is odd. Then, on general symmetry grounds, the coupling between the electrons and the e_c mode would be expected to produce a nonvanishing matrix element coupling the S_1 and the S_2 states, leading eventually to an avoided crossing between the corresponding bands, with a gap between the two proportional to the effective interband tunneling amplitude [6]. As a consequence of that mixing, the adiabatic description in terms of uncoupled BO surfaces would lose meaning, and the quantum nature of the phonons should be included explicitly. However, in absence of the g^0 -term, the Hamiltonian possesses a subtle electronic symmetry (particle-hole P_{ph}) which leads to the vanishing of the interband tunneling matrix element, even for $e_c \neq 0$, as explained below. P_{ph} is defined as the invariance of H (when $g^0 = 0$, and up to an inessential chemical potential shift) under the transformation $f_{i\uparrow}^\dagger \rightarrow (1)^i f_{i\uparrow}$. Taking into account that the electronic states in polyenes correspond to half-filled configurations (the number of \uparrow -electrons $N = L$) and that this subspace is left invariant by P_{ph} , the eigenstates of H within this sector can be classified as even or odd according to P_{ph} [9]. Detailed analysis reveals that S_1 is even under P_{ph} , while S_2 is odd. As a consequence, the interaction term g alone cannot produce the interband coupling leading to the non-adiabatic effects observed in these molecules.

Role of g^0 . For this reason, the additional interaction g^0 , which breaks particle-hole symmetry, is essential for the internal conversion in our model. Fig. 1(d) shows the BO energy surfaces when g^0 is included. Notice that the ground state energy surface is practically unaffected by this interaction. This is due to the fact that the on-site Coulomb repulsion inhibits charge fluctuations in the ground state, thus making the g^0 term, involving the net charges q_i , ineffective. On the contrary, charge fluctuations are important in the excited states, and couple to the phonon modes through the g^0 term: As a consequence of the quantum tunneling for $e_c \neq 0$, due to g^0 , the two relevant potential-energy surfaces show now an avoided crossing (Fig. 1(d)), instead of intersecting (Fig. 1(c)). A rough estimate for the strength of g^0 can be obtained from its effect on a C₂ dimer. By fitting experimental data for the bond lengths of C₂ (1.2425 Å) and of C₂ (1.2682 Å) with our model, we get $g^0 = 3.95$ eV/Å [13].

An alternative rough estimate based on the ionic radii of C^{+4} and C^{-4} ions (0.15 and 2.60 Å respectively [14]), leads to $g^0 \approx 10$ eV/Å. We found that $g^0 \approx 5$ eV/Å leads to reasonable values for the effective interband coupling and for the position of the conical intersection.

In order to describe the observed internal conversion effects, the adiabatic picture must be abandoned. The normal coordinates are quantized as: $e_a = \frac{1}{\sqrt{\hbar=2m}} (a + a^\dagger)$; $e_c = \frac{1}{\sqrt{\hbar=2m}} (c + c^\dagger)$. The resulting Hamiltonian H can be numerically diagonalized by introducing a cutoff in the number of phonons n_a and n_c . We found that keeping states with up to $n_a = n_c = 10$ was enough to obtain accurate results.

The laser pump is simulated by acting at $t = 0$ on the ground state $|j_0\rangle$ with the following operator:

$$\hat{O} = \sum_m \sum_i G_m |j_m\rangle \langle j_0| \hat{E}_i^\dagger; \quad (2)$$

where $|j_m\rangle$ denote the exact eigenstates of H , and the effect of the laser electric field is represented by the dipole operator $\hat{E} = \sum_i R_i q_i$, where R_i is the position of the C atom i for $u_i = 0$. The pump pulse is assumed to have a Gaussian shape in time. The Fourier transform of its envelope determines the excitation amplitudes $G_m = \exp(-\frac{(\omega_m - \bar{\omega})^2}{2\sigma^2})$, where $\omega_m = E_m - E_0$ are the excitation energies relative to the ground state E_0 , while $\bar{\omega}$ and σ are the mean excitation energy and the energy spread of the pump pulse. The Schrodinger time evolution of the prepared wave packet is then given by: $|j(t)\rangle = \exp(iHt) \hat{O} |j_0\rangle$. A qualitative picture of the resulting dynamics can be obtained from $P_o(t) = \langle j(t) | \hat{P}_o | j(t) \rangle$, where \hat{P}_o is defined as the projector of the eigenstates of H on the subspace of electronic states with odd parity under space inversion. $P_o(t)$ is shown in Fig. 2. The first two singlet excitation energies (with predominantly S_1 and S_2 character) are 3.74 eV and 4.31 eV respectively. The spectral density profile of the initial wave packet is shown in the inset of Fig. 2 for a pulse with $\sigma = 2$ eV and $\bar{\omega} = 4.3$ eV. The results for $P_o(t)$ in Fig. 2 show that, on top of a fast oscillatory component, there is a slower internal conversion component which lasts approximately 243 fs. This process is dominated by the two excited states labelled by (1) and (2) in the inset of Fig. 2. The excitation energies of these states are $\omega_1 = 4.304$ eV and $\omega_2 = 4.315$ eV, respectively. State (1) has predominantly S_1 (even) character ($\langle j_1 | \hat{P}_o | j_1 \rangle = 0.4$), while state (2) has predominantly S_2 (odd) character ($\langle j_2 | \hat{P}_o | j_2 \rangle = 0.74$). The evolution of a wave packet composed by just these two states is indicated with a dashed line in Fig. 2. This behavior suggests that the relevant time scale in the evolution of $|j(t)\rangle$ is set by $\hbar/(\omega_2 - \omega_1)$.

Within the sudden approximation, the photoelectron spectrum at time t is essentially a measure of the following spectral function [15]

$$I(t) = \sum_{i,j} \sum_m \langle j_m | \hat{E}_i^\dagger | j(t) \rangle \langle j | \hat{E}_i | j_m \rangle \exp(-i(E_m - E_j)t); \quad (3)$$

where E_m^0 and $|j_m^0\rangle$ denote the eigenenergies and eigenstates of H upon removal of a valence electron. Results for the time evolution of $I(t)$ are shown in Fig. 3, where an artificial broadening of the delta-functions has been introduced. The most salient feature of Fig. 3 is the transfer of spectral weight, as a function of time, from a group of states close in energy to the ground state of the system with $N = L - 1$ electrons (all of them with a predominantly D_0 nature, i.e. a doublet obtained by photoexciting S_2 [5]), to a group of states at a higher energy. The latter states are identified as vibrationally hot states with predominantly D_1 nature (obtained by photoexciting S_1). The arrow in the lowest panel of Fig. 3 indicates the position of the lowest-energy state related to such a band. The behavior of the photoelectron spectra as a function of time is in qualitative agreement with the experimental results of TRPS. The larger energy gap between the relevant photoelectron spectral features which we find in our simulation (2 eV in our case, to be compared with the experimental result of 1.2 eV [5]) should be likely ascribed to the smaller size of the molecule we are considering in our simulation.

In summary, we have shown that the model Hamiltonian in Eq. (1) contains all the basic ingredients which are necessary to explain the essential features of the dynamics of linear polyenes, notably electron-electron and electron-phonon interactions treated in a non-adiabatic (fully quantum) framework. With such a model, we have described in detail the various features of a time-resolved photoemission spectroscopy experiment, obtaining a good picture of the underlying physics. We remark that, although the ground state properties as well as the structure of the electronic excited states are properly described by the standard PPPP model [9,10], the proper treatment of the observed non-adiabatic internal conversion, related to tunneling between coupled Born-Oppenheimer states, requires the inclusion of usually neglected electron-phonon interactions, such as the g^0 term we have considered, which break a residual particle-hole symmetry of the Hamiltonian. On the technical side, we remark that exact diagonalization techniques are useful theoretical tools for the study of these effects, as shown by the reasonable agreement of our simulations with the behavior reported in Ref. [5].

We thank P. Bolcatto for useful discussions. LA and AAA acknowledge support from CONICET. Part of the numerical work was done at the Max Planck Institut PKS.GES acknowledges support by MIUR under project COFIN.

- (¹) Permanent address: Departamento de Física, Universidad de Buenos Aires, Ciudad Universitaria Pabellón I, (1428) Buenos Aires, Argentina.
- [1] J. Michl and J. Bonacic-Koutecky, *Electronic Aspects of Organic Photochemistry*, (Wiley, New York, 1990).
- [2] R. W. Schoenlein, L. A. Peteanu, R. A. Mathies, and C. V. Shank, *Science* 254, 412 (1991).
- [3] J. Jortner and M. A. Ratner, *Molecular Electronics* (IUPAC, Blackwell, Oxford, 1997).
- [4] W. Radlo et al, *Chem. Phys. Lett.* 281, 20 (1997); D. R. Cyr and C. C. Hayden, *Chem. Phys. Lett.* 281, 20 (1997); V. Blanchet and A. Stolow, *J. Chem. Phys.* 108, 4371 (1998).
- [5] V. Blanchet, M. Zgierski, T. Seideman and A. Stolow, *Nature* 401, 52 (1999).
- [6] I. B. Bersuker and V. Z. Polinger *Vibronic Interactions in Molecules and Crystals*, Springer-Verlag (1989).
- [7] M. Seeland W. Domcke, *J. Chem. Phys.* 95, 7806 (1991); A. Kuhl and W. Domcke, *J. Chem. Phys.* 116, 263 (2002).
- [8] A. W. Marshall and M. Karplus, *J. Am. Phys. Soc.* 96, 5612 (1972).
- [9] W. Barford, R. J. Bursill, and M. Y. Lavrentiev, *Phys. Rev. B* 63, 195108 (2001).
- [10] G. Rossi and W. Schneider, *J. Chem. Phys.* 104, 9511 (1996).
- [11] F. Zerbetto, M. Zgierski, F. Negri and G. Orlandi, *J. Chem. Phys.* 89, 3681 (1988).
- [12] W. G. Bouwman et al, *J. Chem. Phys.* 94, 7429 (1990).
- [13] K. P. Huber and G. L. Hersberg, *Molecular spectra and molecular structure IV. Constants of Diatomic Molecules* (Van Nostrand Reinhold, New York, 1979).
- [14] T. Slabaugh and D. Parsons, *General Chemistry*, John Wiley and sons, New York, 1966.
- [15] A. L. Fetter and J. D. Walecka, *Quantum theory of many particle systems*, San Francisco: McGraw-Hill (1971).

FIG. 1. (a) Scheme of the linear polyene. Carbon and Hydrogen atoms are denoted by C and H respectively. (b) Scheme of the normal modes of the molecule. (c) Cuts of the potential energy surfaces for $g^0 = 0$, with $t_0 = 2$ eV, $U = 4.2$ eV, $g = 3$ eV/Å, $K = 36$ eV/Å². Dashed and solid lines correspond to $e_c = 0; 0.1$, respectively. (c) Same as (b) for $g^0 = 5$ eV/Å.

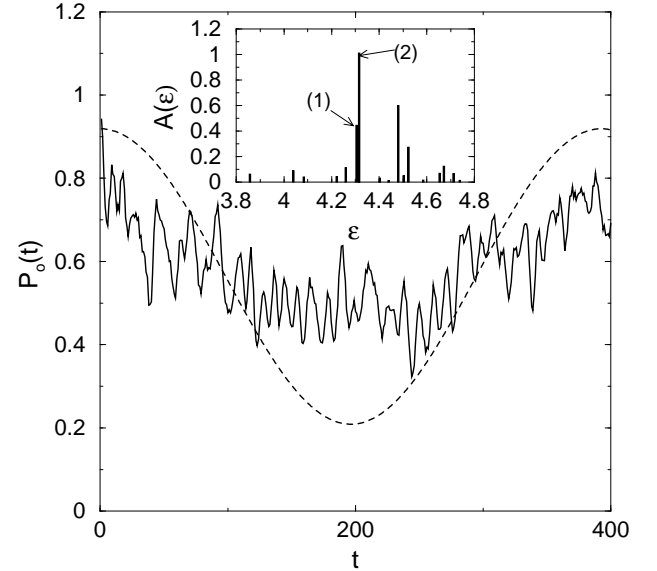
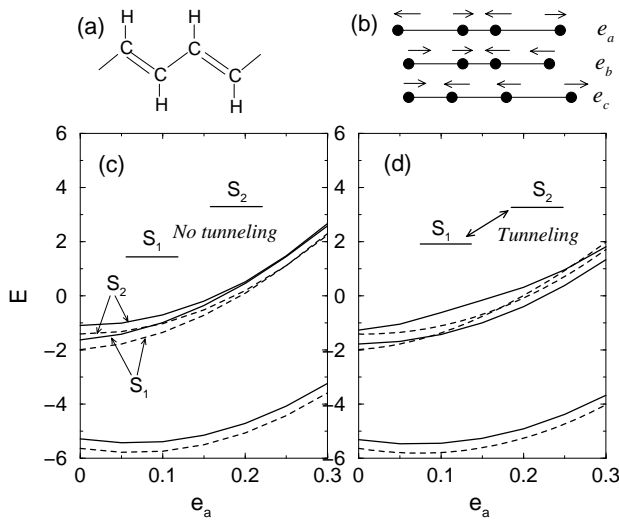


FIG. 2. Evolution of the projector $P_0(t)$ (Solid line). The model parameters are those of Fig. 1 (c). Dashed line: evolution of $P_0(t)$ for a wave packet consisting of the two states (1) and (2) indicated in the inset. Inset: Spectrum of the prepared wave packet for a Gaussian laser pump pulse with $\bar{\omega} = 4.3$ eV and $\sigma_p = 2$ eV.



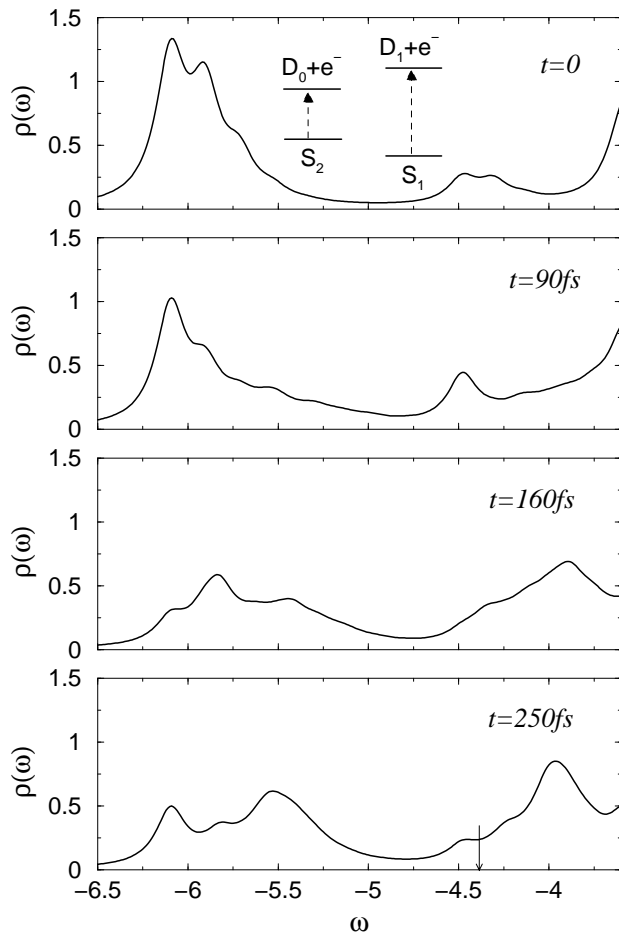


FIG. 3. Evolution of the photoelectron spectra for the prepared wave packet of Fig. 2.